Connecting Packing Efficiency of Binary Hard Sphere Systems to Their Intermediate Range Structure

Houfei Yuan,[1] Zhen Zhang,[2] Walter Kob,[3,1,*] and Yujie Wang[1,†]
[1]School of Physics and Astronomy, Shanghai Jiao Tong University, Shanghai 200240, China
[2]Center for Alloy Innovation and Design, State Key Laboratory for Mechanical Behavior of Materials, Xi'an Jiaotong University, Xi'an 710049, China
[3]Laboratoire Charles Coulomb, University of Montpellier and CNRS, F-34095 Montpellier, France

(Received 31 August 2021; revised 9 November 2021; accepted 1 December 2021; published 27 December 2021)

Using computed x-ray tomography we determine the three dimensional (3D) structure of binary hard sphere mixtures as a function of composition and size ratio of the particles q. Using a recently introduced four-point correlation function we reveal that this 3D structure has on intermediate and large length scales a surprisingly regular order, the symmetry of which depends on q. The related structural correlation length has a minimum at the composition at which the packing fraction is highest. At this composition also the number of different local particle arrangements has a maximum, indicating that efficient packing of particles is associated with a structure that is locally maximally disordered.

DOI: 10.1103/PhysRevLett.127.278001

Hard sphere (HS) systems play a paramount role in statistical mechanics and material science since they are important models to study the behavior of many-particle systems like liquids, colloids, and metallic glasses [1–4]. Also in the domain of granular materials many experimental and theoretical studies have used HS-like systems since granular particles usually have a high modulus and the simplicity of the particle shape allows us to probe the influence of friction and roughness on the properties of granular assemblies [5,6]. Since for HS the interaction energy between the particles is trivial, the properties of such systems is encoded in their structure and hence many previous studies have aimed to characterize it on various length scales [1,4,5,7,8]. Many of these investigations focused on one-component systems since this choice facilitates the description of the packing structure [1,7]. However, in the context of the glass transition one also often uses weakly polydisperse samples or a slightly asymmetric binary mixture, since this suppresses the crystallization of the liquid while keeping its structure close to the well understood one-component case [9,10]. These studies have shown that, depending on the composition and the packing fraction, the local structure, i.e., the first nearest neighbor shell, shows a surprisingly rich variety [10–15]. In contrast to these almost one-component systems, the case of mixtures in which the particles have a size ratio that differs significantly from unity has been studied much less [16–22]. Understanding this structure is, however, important since such highly asymmetric systems are relevant for describing the behavior of real granular materials, which are usually highly polydisperse, as well for the glass-forming ability of multicomponent systems like metallic glasses in which the atoms can have very different radii [23–29]. In addition it has recently been found that such strongly asymmetric mixtures can have local structures with unexpected symmetries which can, e.g., be used to create novel materials via self-assembly [30]. The main reason for our lack of understanding of these systems is that their theoretical description is significantly more complex and experiments on colloidal systems are hampered by the precise control of size ratio, while granular systems are prone to the phenomenon of phase separation [31,32]. A further problem that one faces with these systems is the difficulty to characterize their structure on intermediate length scales since the presence of two particle sizes gives rise to a highly complex distance dependency of the partial radial distribution functions, i.e., the standard quantities that are used to characterize the structure of many-body systems [19,33–35]. Because of these difficulties there is at present little insight on how the size ratio or the composition affects the packing density or the structure of asymmetric HS systems.

In this work we use the computed tomography (CT) technique to probe how composition and size ratio affect the packing fraction of a binary granular system. Using a recently developed method to characterize the structure of disordered systems at intermediate and large length scales we are able to show that a high packing fraction is intimately related to the presence of a short structural correlation length.

Our system is a binary mixture of particles (acrylonitrile butadiene styrene plastic), denoted in the following as "big" (b) and "small" (s) particles, with size ratio $q = d_b/d_s$, where d_b and $d_s = 3.0$ mm are the respective diameters. The number fraction of small particles will be denoted by x. We consider two size ratios: $q = 1.33$, which corresponds

to a mixture that has particles with similar size, and $q = 2.0$, i.e., the particle sizes are significantly different. The particles are mixed and then poured into a cylinder (diameter is 180 mm and filling height is 200 mm), the walls of which have been covered randomly with half spheres of diameter 4 mm to prevent layering of the particles. Subsequently, the cylinder is placed in a medial CT scanner and the particle positions are obtained with a precision of about $0.01 d_s$. More details on the experimental procedure are given in Supplemental Material (SM) [36]. Depending on the concentration x we have between 22 000 and 169 000 particles in the cylinder.

We analyze the 3D structure of the samples by introducing a local coordinate system [42]. For this, one picks any three particles of the same type and which are nearest neighbors, see SM [36], Fig. S5(a). We define the position of particle No. 1 as the origin, the direction from particle No. 1 to No. 2 as the z axis, the plane containing the three particles as the x-z plane and the y axis is orthogonal to it. This local reference frame allows us therefore to determine the 3D distribution of the particles that have a distance r from the central particle, i.e., a four-point correlation function.

In Fig. 1(a) we show for different values of r the distribution $\rho_{bb}(\vec{r})$, i.e., the 3D distribution of the density of the b particles if at the center we also have a b particle ($q = 1.33$ and $x = 0.47$). The snapshots demonstrate that $\rho_{bb}(\vec{r})$ is highly anisotropic in that it shows, at a given r,

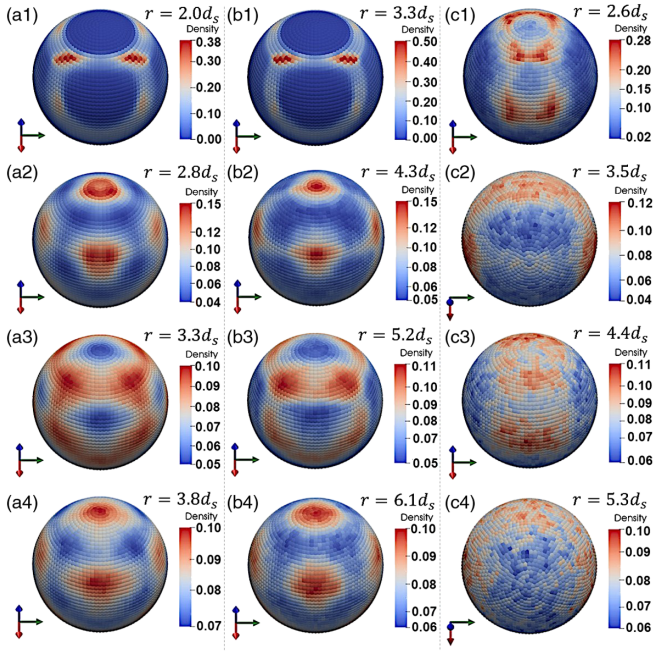

FIG. 1. Distribution of particles in three dimensions in a shell of thickness 0.5 d_s. (a1)–(a4) bb correlation for the $x = 0.47$ mixture ($q = 1.33$ system); (b1)–(b4) bb correlation for the $x = 0.55$ mixture ($q = 2.0$ system); (c1)–(c4) sb correlation for the $x = 0.55$ mixture ($q = 2.0$ system).

spots of high intensity that are arranged in a regular manner on the surface of the sphere. Depending on r, the geometrical arrangement of these spots has an icosahedral symmetry, Figs. 1(a2) and 1(a4) or a dodecahedral one, Figs. 1(a1) and 1(a3), with the high intensity spots for one symmetry corresponding to the low intensity spots in the other one, i.e., the two symmetries are dual (see SM [36]). This result is reasonable since the local wells formed by three neighboring particles at a given r will give rise to a high density at the distance of the subsequent layer [42]. Our finding regarding this regular alternation between these two platonic symmetries is thus the first experimental evidence that the structural order found in Ref. [42] does indeed exist in real systems. We also mention that the same alternating sequence is found for other compositions and other types of density fields [e.g., $\rho_{sb}(\vec{r})$, in which one has a s particle in the center], although the symmetries of the structure might be a bit more fuzzy.

For the $q = 2.0$ system the field $\rho_{bb}(\vec{r})$ is shown in Fig. 1(b) and one sees that the spatial distribution is similar to the one of the $q = 1.33$ system, i.e., two alternating symmetries that are dual to each other. Figure 1(c) show that if the central particle is a s particle, the density field has no longer an icosahedral-dodecahedral symmetry, although one still recognizes the presence of two alternating symmetries with increasing r. The first pattern has two zones of high intensities on the left and right of the sphere surface, connected by a broad band at the top of the sphere [Figs. 1(c2) and 1(c4)] while the second pattern has three prominent bands orthogonal to the x-z plane [Figs. 1(c1) and 1(c3)], see Movie 1 in Supplemental Material [36]. Thus, these two spatial distributions have less symmetry than the ones found for $q = 1.33$, indicating that increasing q results in a decrease of the order at intermediate and large r.

The standard way to characterize the structure of many-body systems is by means of the partial radial distribution functions $g_{\alpha\beta}(r)$, with $\alpha, \beta \in \{b, s\}$, or the partial static structure factors [3]. Supplemental Material Figs. S5 and S6 [36] show that for $q = 2.0$ it is difficult to interpret the r dependence of these functions due to the presence of a multitude of peaks, the height of which show a complicated r dependence, in agreement with previous studies [19,34,35]. Since also the dependence of $g_{\alpha\beta}(r)$ on composition is complex, Fig. S6, it is not possible to extract from these functions a physically meaningful decay length that could be used to describe the range of the structural order. Hence, one concludes that the projection of the complex 3D structure found in Fig. 1 on the one-dimensional quantity $g_{\alpha\beta}(r)$ leads to a severe loss of information and thus it is necessary to study directly the four-point correlation function.

To quantify the anisotropic density distribution $\rho_{\alpha\beta}(\vec{r})$ we decompose it into spherical harmonics $Y_l^m(\theta, \phi, r)$: $\rho_{\alpha\beta}(\theta, \phi, r) = \sum_{l=0}^{\infty} \sum_{m=-l}^{l} \rho_{\alpha\beta,l}^m(r) Y_l^m(\theta, \phi)$, where θ

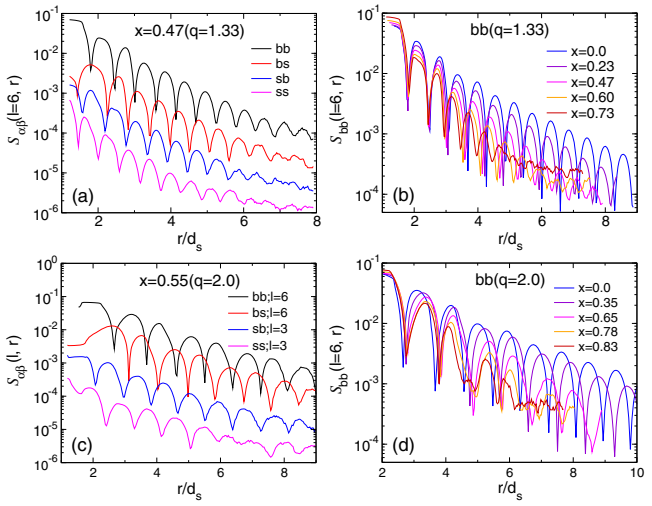

FIG. 2. $\mathcal{S}_{\alpha\beta}(l,r)$ for bb, bs, sb, and ss correlations. Curves in panels (a) and (c) are shifted vertically by powers of 10^{-1} (top to bottom). (a) and (c) Different correlations for the $q = 1.33$ and $q = 2.0$ systems, respectively. (b) and (d) bb correlation for different concentrations x for the $q = 1.33$ and $q = 2.0$ systems, respectively.

and ϕ are the angular variables and the expansion coefficients $\rho^m_{\alpha\beta,l}$ are given in SM [36]. We then use the square root of the angular power spectrum, $\mathcal{S}_{\alpha\beta}(l,r) = [(2l+1)^{-1}\sum_{m=-l}^{l}|\rho^m_{\alpha\beta,l}(r)|^2]^{1/2}$, to characterize the anisotropy of the density distribution.

Figure 2(a) presents for $q = 1.33$ and $x = 0.47$ the r dependence of $\mathcal{S}_{\alpha\beta}$ for the four possible combinations of the field. These curves are for $l = 6$, since $\mathcal{S}_{\alpha\beta}(l = 6, r)$ has the largest signal (see SM [36]) due to the large number of angles around 60° in the icosahedron (dodecahedron)-like structure of the density field, see Fig. 1(a). We see that these functions show an oscillatory behavior with an envelope that decays in an exponential manner, in agreement with the results from Ref. [42] where the origin of these oscillations have been discussed. Thus, the slope of the envelope can be used to define a structural length scale ξ which will be studied in the following. Since this slope is independent of the function considered (see SM [36]), we discuss in the following its average value ξ.

Figure 2(b) shows $\mathcal{S}_{bb}(r)$ for the $q = 1.33$ system at different concentrations x and one sees that the position of the peaks depends only mildly on x but that their intensity changes rapidly with increasing x. This indicates that the geometry of the structure, i.e., the icosahedron-dodecahedron sequence, is present up to relatively high concentration of the small particles, but that the structures are less pronounced.

Figure 2(c) shows $\mathcal{S}_{bb}(r)$ for the $q = 2.0$ system at $x = 0.55$. The value of l is also 6, since the signal is again the strongest. However, if the coordinate system is centered on a s particle we find that the functions $\mathcal{S}_{s\alpha}(r)$ have the largest signal for $l = 3$, a result that is consistent with the fact that the density field is no longer given by an icosahedra-dodecahedral symmetry, see Fig. 1(c). Despite the different values for l, we see that the decay length of the signal is independent of the field considered and thus can be used as a robust indicator for the structural order.

Figure 2(d) shows $\mathcal{S}_{bb}(r)$ for the $q = 2.0$ system for different values of x. We recognize that the x dependence of the curves is smooth and that the main effect of changing composition is that the slope of the envelope changes and is nonmonotonic in x. Thus, we can conclude that, in contrast to the partial radial distribution functions $g_{\alpha\beta}(r)$, the quantity $\mathcal{S}_{\alpha\beta}(l,r)$ allows us to quantify in a direct manner how the structure on intermediate and large scale evolves with composition.

Figure 3(a) shows the x dependence of the length scale ξ for the $q = 1.33$ system and one recognizes that ξ^{-1} shows a maximum at around $x_{\max} = 0.7$, i.e., at this concentration the structure is maximally disordered. [Note that here we express ξ in terms of the mean particle diameter $d_{\text{mean}} = (1-x)d_b + xd_s$ so that the $x = 0$ and $x = 1$ systems have the same normalized length scale.] For (quasi-)one-component systems it is common to determine the structural coherence length from σ_S, the width of the first peak in the static structure factor [2]. In SM [36] we show that this is indeed feasible for the $q = 1.33$ system while for larger q this is not possible since there is not always a main peak. Also included in Fig. 3(a) is the x dependence of σ_S and one recognizes that this data is qualitatively very similar to the one of ξ^{-1} giving evidence that these two quantities are indeed closely related to each other. Also shown in the graph is the packing fraction φ defined by $\varphi = \sum_i v_i / \sum_i v_{\text{voro},i}$, where v_i and $v_{\text{voro},i}$ are, respectively, the volume and radical Voronoi volume of particle i [43]. Since $\varphi(x)$ shows a maximum close to $x_{\max}$ we have a first indication that a small correlation is associated with a high packing fraction.

For the $q = 2.0$ system, Fig. 3(b), we find that ξ^{-1} has a maximum which is shifted to larger x, i.e., $x_{\max} \approx 0.8$, and also the maximum of the packing fraction moves to larger x

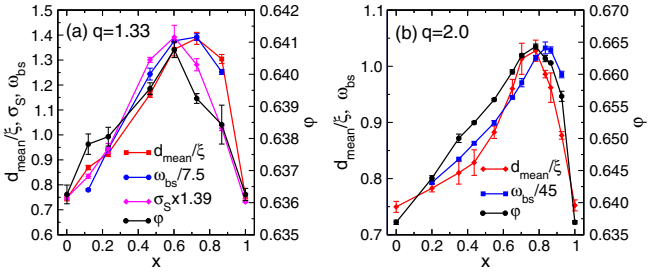

FIG. 3. Composition dependence of the length scale ξ for the $q = 1.33$, panel (a), and $q = 2.0$, panel (b), systems. Also included is the packing fraction φ, the standard deviation of the coordination number ω_{bs} and in panel (a) the full width at half maximum of the static structure factor, σ_S.

and its height is increased, consistent with theoretical predictions [17,20,21]. In agreement with the results for the $q = 1.33$ system, the location of the maximum in $\varphi(x)$ coincides with the one of ξ^{-1}, giving further evidence that these two quantities are closely related.

To understand the connection between φ and ξ one has to recall that one-component HS-like systems can have a *local* packing fraction that is significantly higher than the *global* packing fraction in that, e.g., the central particle of an icosahedron has $\varphi_{\mathrm{ico}} = 0.74$, thus well above the density of random close packing, $\varphi_{\mathrm{rcp}} \approx 0.64$ [2]. The reason for this difference is that icosahedra cannot tile space and hence the densely packed local structures have to be supplemented with structures that are packed less densely, making that $\varphi_{\mathrm{rcp}} < \varphi_{\mathrm{ico}}$ [1,2]. The presence of a second kind of particle has two effects on the packing. (1) Big particles can increase their local packing density by having small particles as nearest neighbors since the minimum distance between a big and small particle is less than the one between two b particles, resulting in a decrease of the Voronoi volume. (Note that we refer here to "nearest neighbors" as the particles sharing a face in the radical Voronoi cell, and this should not be confused with particles at contact, see SM [36] for details.) This trend is shown in Fig. 4 for the two systems in that we find a slow rise of φ_b with x and the increase is faster for large q. (2) For small particles the presence of the b particles has the opposite effect, i.e., the local packing fraction $\varphi_s(x)$ decreases with the addition of the big particles because a big particle that is close to a small one will strongly increase the Voronoi volume of the latter, see Fig. 4. The total packing fraction is given by

$$\varphi(x) = \frac{N_b S_b + N_s S_s}{N_b V^b_{\mathrm{voro}} + N_s V^s_{\mathrm{voro}}} = \frac{\varphi_b(x)\varphi_s(x)[q^3(1-x)+x]}{\varphi_s(x)q^3(1-x)+\varphi_b(x)x}, \tag{1}$$

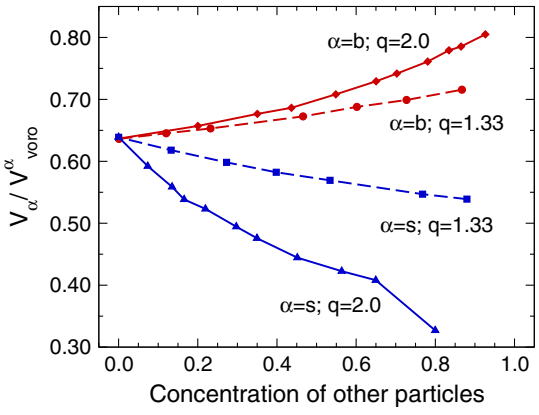

FIG. 4. Average local packing fraction φ_b and φ_s. Full and dashed lines are for the $q = 2.0$ and $q = 1.33$ systems, respectively. Error bars are smaller than the size of the symbols.

where N_α and S_α are the number and volume of particles of type α, respectively. Since φ_s shows a stronger x dependence than φ_b, one has a maximum in $\varphi(x)$ at $x_{\mathrm{max}} > 0.5$, in agreement with the data from Fig. 3.

Note that φ_b (and φ_s) is an average packing fraction, i.e., it is the weighted average over particles that have different local environments. In order to maximize φ_b one thus needs that the local environments that are frequent do (i) have a high packing fraction and (ii) can be joined together without loosely packed interfaces between them. This latter condition is met most easily if there is a large number of possible local environments that have a high packing density since this allows for a greater flexibility in the assembly of the global packing. To estimate the number of such local environments at a given x we probe $C_{\alpha\beta}(k)$, the probability that a particle of type α has exactly k nearest neighbors of type β. Figure S13 shows that these distributions are Gaussian-like and thus their standard deviation $\omega_{\alpha\beta}$ can be taken as a measure for the variety of the local environments of a given particle type. The x dependence of ω_{bb} is included in Fig. 3 as well and one sees that this curve does indeed match very well the x dependence of φ. [Figure S14 demonstrates that the shape of $\omega_{\alpha\beta}(x)$ is independent of the choice of α and β and Fig. S15 that the statistically relevant local environments do indeed have a high packing fraction.] Thus, this supports the view that in order to have a high packing fraction one needs indeed a large variety of local structures since this allows us to create a packing that has high density everywhere. Since these local structures are by definition different, the resulting global structural correlation length will be small. Hence, this rationalizes why $\varphi(x)$ and ξ^{-1} peak at the same concentration x_{max}, see Fig. 3.

In this work we have used a CT scanner to determine the structural properties of granular packings on intermediate and large length scales. Because of the preparation protocol and the existence of friction, these structures are not exactly the same as the frictionless packings studied in theoretical works [16,20,21], but they do correspond to packings that occur in real granular systems. Using a novel method to characterize the structure in 3D, we are able to determine for the first time a static length scale ξ even for strongly asymmetric mixtures. The fact that $\xi^{-1}(x)$ shows a maximum at the same concentration at which the maximum packing fraction occurs indicates that in multicomponent disordered systems efficient packing is related to a *short* correlation length. Surprisingly, the presence of a short correlation length does not exclude the possibility that the structure shows order even on intermediate length scales, see Fig. 1. The nature of this order depends on q and can be expected to influence the glass-forming ability of the system [44,45], calling for further studies to clarify this dependence. Note that the presence of the symmetry shown in Fig. 1(c) has not been documented before, demonstrating that probing the structure in 3D is a powerful approach

which allows to characterize the structure of many-body systems that so far could not be described in an insightful manner. Exploiting this approach to multicomponent systems will thus allow not only to advance our understanding of disordered systems but also facilitate the creation of novel self-assembled materials and glass-forming systems [30].

Finally, we mention that our result on the existence of a maximum in $\varphi(x)$, directly related to the competition between opposite trends for the local packing density of the big and small particles, calls for studies that connect this observation to the formalism of the Edwards measure for granular systems [6,46]. Since this measure is based on the entropy related to the global packing density, it is important to probe how the mentioned opposite trends are reflected in this theoretical framework, i.e., to see whether it is possible to rationalize our results within a thermodynamic approach.

We thank H. Tanaka and F. Zamponi for useful discussions. W. K. is senior member of the Institut Universitaire de France. The work was supported by the National Natural Science Foundation of China (No. 11974240), the Shanghai Science and Technology Committee (No. 19XD1402100), and the China Scholarship Council Grant No. 201606050112.

H. Y. and Z. Z. contributed equally to this work.

*walter.kob@umontpellier.fr
†yujiewang@sjtu.edu.cn

[1] G. Parisi and F. Zamponi, Rev. Mod. Phys. **82**, 789 (2010).
[2] K. Binder and W. Kob, *Glassy Materials and Disordered Solids: An Introduction to Their Statistical Mechanics* (World Scientific, Singapore, 2011).
[3] J.-P. Hansen and I. R. McDonald, *Theory of Simple Liquids* (Academic Press, New York, 2013).
[4] S. Torquato, *Random Heterogeneous Materials: Microstructure and Macroscopic Properties* (Springer, New York, 2002).
[5] C. Song, P. Wang, and H. A. Makse, Nature (London) **453**, 629 (2008).
[6] Y. Yuan, Y. Xing, J. Zheng, Z. Li, H. Yuan, S. Zhang, Z. Zeng, C. Xia, H. Tong, W. Kob, J. Zhang, and Y. Wang, Phys. Rev. Lett. **127**, 018002 (2021).
[7] K. Watanabe and H. Tanaka, Phys. Rev. Lett. **100**, 158002 (2008).
[8] S. Torquato and F. H. Stillinger, Rev. Mod. Phys. **82**, 2633 (2010).
[9] W. Kob and H. C. Andersen, Phys. Rev. E **51**, 4626 (1995).
[10] H. Tong and H. Tanaka, Phys. Rev. X **8**, 011041 (2018).
[11] M. Clusel, E. I. Corwin, A. O. Siemens, and J. Brujić, Nature (London) **460**, 611 (2009).
[12] D. Coslovich and G. Pastore, J. Chem. Phys. **127**, 124504 (2007).
[13] C. P. Royall and S. R. Williams, Phys. Rep. **560**, 1 (2015).
[14] R. S. Farr and R. D. Groot, J. Chem. Phys. **131**, 244104 (2009).
[15] V. Ogarko and S. Luding, Soft Matter **9**, 9530 (2013).
[16] J. Dodds, Nature (London) **256**, 187 (1975).
[17] P. Richard, L. Oger, J. Troadec, and A. Gervois, Physica (Amsterdam) **259A**, 205 (1998).
[18] P. Richard, L. Oger, J. Troadec, and A. Gervois, Eur. Phys. J. E **6**, 295 (2001).
[19] A. Statt, R. Pinchaipat, F. Turci, R. Evans, and C. P. Royall, J. Chem. Phys. **144**, 144506 (2016).
[20] M. Danisch, Y. Jin, and H. A. Makse, Phys. Rev. E **81**, 051303 (2010).
[21] I. Biazzo, F. Caltagirone, G. Parisi, and F. Zamponi, Phys. Rev. Lett. **102**, 195701 (2009).
[22] Y. Yuan, L. Liu, Y. Zhuang, W. Jin, and S. Li, Phys. Rev. E **98**, 042903 (2018).
[23] C. Graf, D. L. Vossen, A. Imhof, and A. van Blaaderen, Langmuir **19**, 6693 (2003).
[24] K. W. Desmond and E. R. Weeks, Phys. Rev. E **90**, 022204 (2014).
[25] S. R. Williams and W. van Megen, Phys. Rev. E **64**, 041502 (2001).
[26] A. Imhof and J. K. G. Dhont, Phys. Rev. Lett. **75**, 1662 (1995).
[27] E. Lázaro-Lázaro, J. A. Perera-Burgos, P. Laermann, T. Sentjabrskaja, G. Pérez-Ángel, M. Laurati, S. U. Egelhaaf, M. Medina-Noyola, T. Voigtmann, R. Castañeda-Priego *et al.*, Phys. Rev. E **99**, 042603 (2019).
[28] J. Bosse and Y. Kaneko, Phys. Rev. Lett. **74**, 4023 (1995).
[29] W. Wang, C. Dong, and C. Shek, Mater. Sci. Eng. R **44**, 45 (2004).
[30] D. Wang, T. Dasgupta, E. B. van der Wee, D. Zanaga, T. Altantzis, Y. Wu, G. M. Coli, C. B. Murray, S. Bals, M. Dijkstra, and A. van Blaaderen, Nat. Phys. **17**, 128 (2021).
[31] G. Seiden and P. J. Thomas, Rev. Mod. Phys. **83**, 1323 (2011).
[32] C. Monteux and F. Lequeux, Langmuir **27**, 2917 (2011).
[33] G. Zerah and J.-P. Hansen, J. Chem. Phys. **84**, 2336 (1986).
[34] C. Grodon, M. Dijkstra, R. Evans, and R. Roth, J. Chem. Phys. **121**, 7869 (2004).
[35] C. Grodon, M. Dijkstra, R. Evans, and R. Roth, Mol. Phys. **103**, 3009 (2005).
[36] See Supplemental Material at http://link.aps.org/supplemental/10.1103/PhysRevLett.127.278001 for details regarding the experimental setup, image processing procedures, and additional calculations, which includes Refs. [37–41].
[37] Y. Cao, J. Li, B. Kou, C. Xia, Z. Li, R. Chen, H. Xie, T. Xiao, W. Kob, L. Hong, J. Zhang, and Y. Wang, Nat. Commun. **9**, 1 (2018).
[38] T. Aste, M. Saadatfar, and T. J. Senden, Phys. Rev. E **71**, 061302 (2005).
[39] M. D. Ediger, J. Chem. Phys. **147**, 210901 (2017).
[40] A. Santos, S. B. Yuste, and M. López de Haro, J. Chem. Phys. **153**, 120901 (2020).
[41] B. Gellatly and J. Finney, J. Non-Cryst. Solids **50**, 313 (1982).

[42] Z. Zhang and W. Kob, Proc. Natl. Acad. Sci. U.S.A. **117**, 14032 (2020).

[43] Since the CT scanner has only a finite spatial resolution, the packing density of the system with only big spheres is not quite the same as the one for a system with the small spheres. In SM [36] we discuss how this minor effect has been corrected.

[44] K. Zhang, W. W. Smith, M. Wang, Y. Liu, J. Schroers, M. D. Shattuck, and C. S. O'Hern, Phys. Rev. E **90**, 032311 (2014).

[45] J. Russo, F. Romano, and H. Tanaka, Phys. Rev. X **8**, 021040 (2018).

[46] S. F. Edwards and R. Oakeshott, Physica (Amsterdam) **157A**, 1080 (1989).